

Magnetohydrodynamic Relaxation Theory

Anthony R. Yeates *

* Durham University, Durham, UK

Abstract

These notes concern the magnetic relaxation problem, in which an electrically-conducting fluid is initialised in some non-trivial state, and is subsequently allowed to relax to some minimum-energy state, subject to the magnetohydrodynamic (MHD) equations. No driving or forcing is applied during this relaxation process, and some form of dissipation allows energy to decrease until the system reaches a relaxed state. Our problem is simple: can we understand or predict this relaxed state?

1 Introduction

We will assume that the dominant form of energy in the system is magnetic, so that the relaxed state is one of *minimal magnetic energy*, subject to some appropriate constraints (much more on these later!). Although we shall also consider the perfectly conducting limit (Section 2.1), resistivity plays an important role, as we shall see. In particular, though many fluids of physical interest have extremely low resistivity, the presence of localised dissipation is nevertheless essential to the global relaxation process.

Although our aim is to keep these notes as general as possible, it is useful to bear in mind the types of physical system where this kind of relaxation process might be relevant. Much of relaxation theory has been developed in the controlled thermonuclear fusion community, notably following the pioneering work of Taylor (Section 2.2). But the constrained minimisation of magnetic energy was already being studied in the astrophysical context in the 1950s, and, since the work of Taylor, there has been much interest in applying similar ideas to astrophysical plasmas in the Sun's atmosphere.

1.1 MHD equations

In these notes, we will assume a conducting fluid that obeys the following MHD equations:

$$\frac{\partial \rho}{\partial t} = -\nabla \cdot (\rho \mathbf{v}), \quad (1)$$

$$\rho \frac{D\mathbf{v}}{Dt} = -\nabla p + \nabla \cdot \overline{\boldsymbol{\sigma}} + \mathbf{j} \times \mathbf{B}, \quad (2)$$

$$\rho \frac{D\epsilon}{Dt} = -p \nabla \cdot \mathbf{v} + (\overline{\boldsymbol{\sigma}} \cdot \nabla) \mathbf{v} + \eta j^2, \quad (3)$$

$$p = \rho \epsilon (\gamma - 1), \quad (4)$$

$$\mu_0 \mathbf{j} = \nabla \times \mathbf{B}, \quad (5)$$

$$\frac{\partial \mathbf{B}}{\partial t} = \nabla \times (\mathbf{v} \times \mathbf{B}) - \nabla \times (\eta \mathbf{j}). \quad (6)$$

Equations (1)-(4) are the usual equations of fluid mechanics for the density ρ , velocity field \mathbf{v} , pressure p and internal energy ϵ , where $\overline{\boldsymbol{\sigma}}$ is the viscous stress tensor and we assume an adiabatic equation of state (4). Compared to a non-conducting fluid, the momentum equation (2) contains an additional Lorentz force $\mathbf{j} \times \mathbf{B}$ due to the magnetic field \mathbf{B} , where \mathbf{j} is the electric current density derived from Ampère's law (5). In (3), there is an additional ohmic dissipation term ηj^2 that corresponds to heating of the fluid by electrical resistivity (we shall assume a uniform resistivity η). The magnetic field \mathbf{B} evolves according to the induction equation (6), which is obtained by substituting the (resistive) Ohm's law into Faraday's law to eliminate the electric field. We assume that the initial magnetic field is divergence-free ($\nabla \cdot \mathbf{B} = 0$), so that it remains so throughout the relaxation thanks to (6).

In principle, we can simply compute the relaxed state by solving these equations as an initial value problem. However, the goal of relaxation theory is to understand what is fundamentally going on when we solve the equations – the “big picture,” if you will. With a deep enough understanding, we may even be able to predict the relaxed state without having to solve the MHD equations at all.

In many astrophysical and laboratory plasmas, we have η very small but non-zero. Accordingly, our aim will be to understand this regime, although we will see along the way what happens in the extreme cases where resistivity is dominant (large η) or vanishing (ideal MHD, $\eta = 0$).

Boundary conditions We shall consider relaxation in a finite domain V . This means that the boundary conditions will play an important role.

We will consider two possible sets of boundary conditions, where we use the notation $B_n \equiv \mathbf{B} \cdot \hat{\mathbf{n}}$ (with $\hat{\mathbf{n}}$ the outward unit normal):

(B1) *Closed field* — $B_n|_{\partial V} = v_n|_{\partial V} = 0$.

(B2) *Line-tied* — $\partial B_n / \partial t|_{\partial V} = 0$ and $\mathbf{v}|_{\partial V} = \mathbf{0}$.

The name “line-tied” comes from the ideal MHD case, where conditions (B2) would imply that magnetic field line footpoints on ∂V cannot move. If $\eta \neq 0$, these footpoints may still move through resistive diffusion.

Initial conditions Except for the requirement that $\nabla \cdot \mathbf{B} = 0$, and possibly boundary condition (B1), we allow for a general initial magnetic field \mathbf{B} . The relaxed state in any particular problem will naturally be dependent on the choice of initial state, or at least on certain properties of it.

1.2 Energy dissipation

Since we are interested in minimizing magnetic energy, it is logical to consider how this evolves. We define the total magnetic energy to be

$$W(t) = \frac{1}{2\mu_0} \int_V B^2 d^3x. \quad (7)$$

Differentiating this expression and using (6), we find that

$$\begin{aligned} \frac{dW}{dt} &= \frac{1}{\mu_0} \int_V \mathbf{B} \cdot \frac{\partial \mathbf{B}}{\partial t} d^3x \\ &= \frac{1}{\mu_0} \int_V \mathbf{B} \cdot \nabla \times (\mathbf{v} \times \mathbf{B} - \eta \mathbf{j}) d^3x \\ &= \frac{1}{\mu_0} \int_V [(\mathbf{v} \times \mathbf{B}) \cdot \nabla \times \mathbf{B} - \eta \mathbf{j} \cdot \nabla \times \mathbf{B}] d^3x \\ &\quad + \frac{1}{\mu_0} \oint_{\partial V} [(\mathbf{v} \times \mathbf{B}) \times \mathbf{B} - \eta \mathbf{j} \times \mathbf{B}] \cdot \hat{\mathbf{n}} d^2x \\ &= - \int_V [\mathbf{v} \cdot (\mathbf{j} \times \mathbf{B}) + \eta j^2] d^3x \\ &\quad + \frac{1}{\mu_0} \oint_{\partial V} [B_n(\mathbf{v} \cdot \mathbf{B}) - v_n B^2 + \eta \mathbf{B} \cdot (\mathbf{j} \times \hat{\mathbf{n}})] d^2x. \quad (8) \end{aligned}$$

Within the volume, this shows that W changes due to both work done against the Lorentz force (which may increase or reduce W), and due to ohmic dissipation (which always reduces W).

The first two boundary terms correspond to bodily transport of magnetic energy into (or out of) V , and both vanish under either (B1) or (B2). The

third term is due to ohmic diffusion through the boundary, and is usually ruled out by additional boundary conditions in practice, in which case

$$\frac{dW}{dt} = - \int_V \left[\mathbf{v} \cdot (\mathbf{j} \times \mathbf{B}) + \eta j^2 \right] d^3x. \quad (9)$$

In the presence of viscosity (the $\overline{\boldsymbol{\sigma}}$ tensor), kinetic energy will eventually dissipate leaving a static equilibrium $\mathbf{v} = \mathbf{0}$. In this situation, magnetic energy will continue to dissipate through ohmic dissipation, toward an asymptotic state where

$$\mathbf{j} = \mathbf{0}. \quad (10)$$

In other words $\nabla \times \mathbf{B} = \mathbf{0}$, which implies that $\mathbf{B} = \nabla\psi$. This is a *potential field*, so-called because $\nabla \cdot \mathbf{B} = 0$ implies that ψ satisfies Laplace's equation $\Delta\psi = 0$. So *unconstrained resistive relaxation leads to a potential field*.

What makes relaxation theory interesting is that a potential field is not usually reached, at least not on a dynamical timescale. Instead, the system settles rapidly into a relaxed state with $\mathbf{v} = \mathbf{0}$, but with $\mathbf{j} \neq \mathbf{0}$. In highly conducting fluids, the remaining ohmic dissipation takes far longer and is often physically irrelevant. The dynamical relaxation phase is what we are really interested in.

Example 1.1 (One-dimensional model; Moffatt 2015). A simple system exhibiting this “two-stage” relaxation process is given by assuming an initial magnetic field $\mathbf{B} = B_0(b_y(x, t)\hat{\mathbf{y}} + b_z(x, t)\hat{\mathbf{z}})$ in a pressureless fluid ($p = 0$) with uniform viscosity μ . For such a magnetic field,

$$\mathbf{j} \times \mathbf{B} = -\frac{\partial p_m}{\partial x} \hat{\mathbf{x}}, \quad (11)$$

where $p_m = B^2/2$ is the magnetic pressure. Thus if $\mathbf{v} = \mathbf{0}$ initially, there will only be a fluid velocity in the x direction, $\mathbf{v} = v(x, t)\hat{\mathbf{x}}$. By defining dimensionless variables $\hat{x} = x/d$, $\hat{t} = t/(\mu/B_0^2)$, $\hat{\rho} = \rho/\rho_0$ and $\hat{\mathbf{b}} = \mathbf{B}/B_0$, the MHD equations reduce to the dimensionless form (dropping the hats)

$$\frac{\partial \rho}{\partial t} = -\frac{\partial}{\partial x}(\rho v), \quad (12)$$

$$\frac{\partial}{\partial t}(\rho v) = -\frac{\partial}{\partial x} \left(\rho v^2 - \frac{1}{\epsilon} \frac{\partial v}{\partial x} + p_m \right), \quad (13)$$

$$\frac{\partial \mathbf{b}}{\partial t} = -\frac{\partial}{\partial x} \left(v \mathbf{b} - \kappa \frac{\partial \mathbf{b}}{\partial x} \right). \quad (14)$$

The dimensionless parameters $\epsilon = \rho_0 B_0^2 d^2 / \mu^2$ and $\kappa = \eta \mu / (B_0^2 d^2)$ are both assumed small, so that the magnetic Prandtl number $\mu / (\rho_0 \eta) = (\epsilon \kappa)^{-1}$ is assumed large.

We can solve equations (12) to (14) numerically using a simple finite-difference method, subject to the boundary conditions

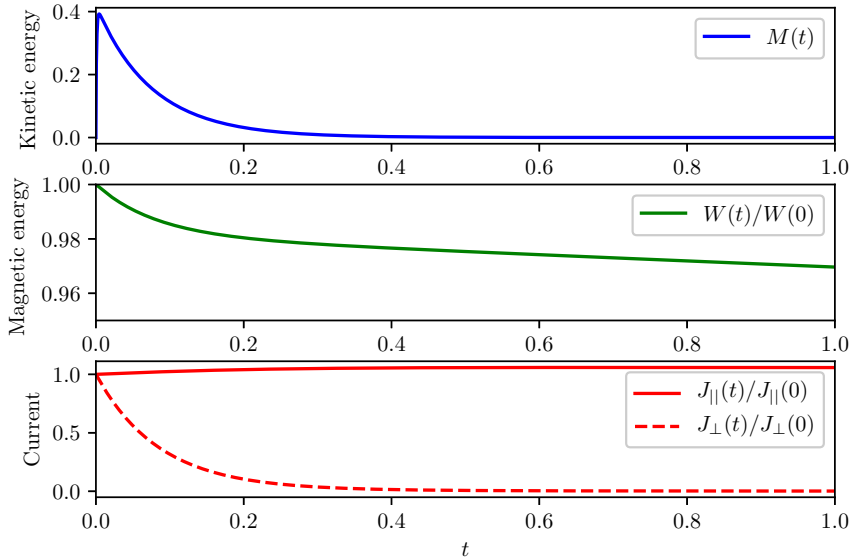
$$\frac{\partial \mathbf{b}}{\partial x}(\pm\pi, t) = \mathbf{0}, \quad v(\pm\pi, t) = 0, \quad (15)$$

although these correspond to neither (B1) nor (B2) above. With $\epsilon = \kappa = 10^{-3}$ and initial conditions

$$\mathbf{b}(x, 0) = 2 \sin(0.1x(3\pi^2 - x^2)) \hat{\mathbf{y}} + 3 \cos(0.1x(3\pi^2 - x^2)) \hat{\mathbf{z}}, \quad (16)$$

$$v(x, 0) = 0, \quad \rho(x, 0) = 1, \quad (17)$$

we obtain the following evolution of the kinetic energy $M(t) = \frac{1}{2} \int_{-\pi}^{\pi} \rho v^2 dx$, magnetic energy $W(t)$, parallel current $J_{\parallel}(t) = \int j_{\parallel} dx$ (with $j_{\parallel} = |\mathbf{j} \cdot \mathbf{B}/B|$) and perpendicular current $J_{\perp}(t) = \int (j - j_{\parallel}) dx$.



The key point here is the presence of an initial dynamical relaxation phase with significant kinetic energy until about $t = 0.5$, followed by a purely resistive decay thereafter. During the initial phase, the perpendicular current is mostly dissipated, but the parallel current is not, so a potential field with $\mathbf{j} = \mathbf{0}$ is not reached until $t \gg 1$. We will see in Section 2.1 that such a force-free state $\mathbf{j} = \alpha(x)\mathbf{B}$ would be expected in an ideal relaxation. It is

notable that α depends on x , so that Taylor's hypothesis (Section 2.2) is not an appropriate model here.

1.3 Topological invariants

To understand the dynamical phase, we need to understand the physical constraints on the fluid, additional to the boundary conditions. In a highly-conducting fluid, these can arise from topological invariants: the magnetic helicities of fluid subvolumes.

Let $V_t \subset V$ be a material volume (moving with the fluid), and let \mathbf{A} be a vector potential for \mathbf{B} , meaning that $\mathbf{B} = \nabla \times \mathbf{A}$. The magnetic helicity in the subvolume V_t , corresponding to this choice of \mathbf{A} , is

$$h(V_t) = \int_{V_t} \mathbf{A} \cdot \mathbf{B} \, d^3x. \quad (18)$$

We can compute the time evolution of this quantity using the transport theorem:

$$\frac{dh(V_t)}{dt} = \int_{V_t} \frac{\partial}{\partial t} (\mathbf{A} \cdot \mathbf{B}) \, d^3x + \oint_{\partial V_t} \mathbf{A} \cdot \mathbf{B} v_n \, d^2x, \quad (19)$$

$$= \int_{V_t} \left(\mathbf{B} \cdot \frac{\partial \mathbf{A}}{\partial t} + \mathbf{A} \cdot \frac{\partial \mathbf{B}}{\partial t} \right) \, d^3x + \oint_{\partial V_t} \mathbf{A} \cdot \mathbf{B} v_n \, d^2x, \quad (20)$$

$$= 2 \int_{V_t} \mathbf{B} \cdot \frac{\partial \mathbf{A}}{\partial t} \, d^3x + \oint_{\partial V_t} \left(\mathbf{A} \cdot \mathbf{B} v_n - \mathbf{A} \times \frac{\partial \mathbf{A}}{\partial t} \cdot \hat{\mathbf{n}} \right) \, d^2x. \quad (21)$$

Uncurling the induction equation (6) shows that

$$\frac{\partial \mathbf{A}}{\partial t} = \mathbf{v} \times \mathbf{B} - \eta \mathbf{j} + \nabla \chi, \quad (22)$$

for some arbitrary scalar potential χ (that depends on the chosen gauge of \mathbf{A}). Substituting this into (21) gives

$$\begin{aligned} \frac{dh(V_t)}{dt} &= 2 \int_{V_t} \left(\mathbf{B} \cdot \nabla \chi - \eta \mathbf{j} \cdot \mathbf{B} \right) \, d^3x \\ &\quad + \oint_{\partial V_t} \left((\mathbf{A} \cdot \mathbf{B}) \mathbf{v} - \mathbf{A} \times (\mathbf{v} \times \mathbf{B}) + \eta \mathbf{A} \times \mathbf{j} - \mathbf{A} \times \nabla \chi \right) \cdot \hat{\mathbf{n}} \, d^2x, \\ &= -2 \int_{V_t} \eta \mathbf{j} \cdot \mathbf{B} \, d^3x + \oint_{\partial V_t} \left[(\chi + \mathbf{v} \cdot \mathbf{A}) B_n - \eta \mathbf{j} \cdot (\mathbf{A} \times \hat{\mathbf{n}}) \right] \, d^2x. \end{aligned} \quad (23)$$

Here we used that $\nabla \cdot \mathbf{B} = 0$ and also that ∂V_t is a closed surface.

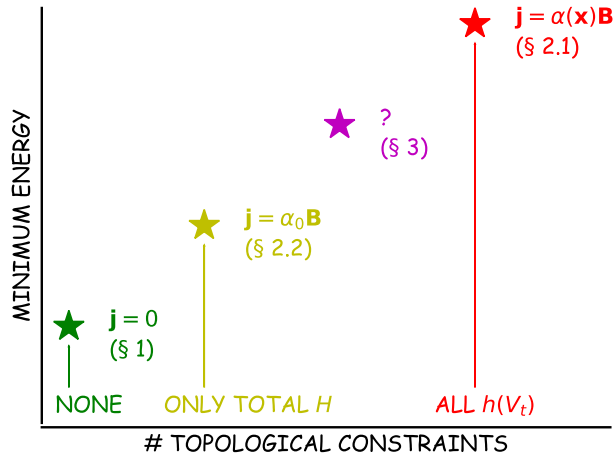
If our fluid were perfectly conducting ($\eta = 0$), then (23) would reduce to the boundary term. Moreover, this boundary term would vanish if $B_n = 0$. So the helicity $h(V_t)$ is invariant under *ideal* MHD whenever V_t is a magnetically-closed subvolume.

When $\eta \neq 0$, then the individual helicities $h(V_t)$ are no longer invariant. In Lecture 3, we will look at what happens to these topological quantities for small but non-zero η .

1.4 Overview of these lectures

We have already seen that the minimum-energy state for an unconstrained resistive relaxation is a potential field with $\mathbf{j} = \mathbf{0}$. In the rest of these notes, we aim to characterise the minimum-energy state reached by the dynamical phase when this is much shorter than the ohmic dissipation timescale.

In relaxation theory, we aim to compute (or at least to characterise) the minimum-energy state in the presence of constraints. Different choices of constraint(s) will lead to different minimum-energy states. The cases that we will study are summarised below:



In Lecture 2, we will consider two well-established cases: (i) ideal MHD where all of the $h(V_t)$ are conserved, and (ii) Taylor relaxation where we impose the much weaker constraint that the total helicity for $V_t = V$ is the only constraint. In both cases, we will see that the minimum-energy

states are force-free fields with $\mathbf{j} = \alpha \mathbf{B}$. The difference is that α must be a constant in case (ii) – a *linear force-free magnetic field* but may be a function of position in case (i) – a *nonlinear force-free magnetic field*.

Lecture 3 describes recent work that aims to better characterise the relaxation process in “realistic” systems that fall somewhere between ideal MHD and Taylor relaxation. The essential idea is to study the evolution of the $h(V_t)$ when the V_t are infinitesimal tubes around each magnetic field line.

2 Traditional Approaches

In this lecture, we discuss two well-studied regimes: ideal MHD and Taylor relaxation.

2.1 Ideal MHD relaxation

In a perfectly conducting fluid with vanishing resistivity ($\eta = 0$), the induction equation (6) simplifies to

$$\frac{\partial \mathbf{B}}{\partial t} = \nabla \times (\mathbf{v} \times \mathbf{B}), \quad (24)$$

which implies that the magnetic field is frozen-in to the fluid (Alfvén’s theorem). As we have seen, the magnetic helicity $h(V_t)$ is then invariant for any magnetically-closed material subvolume V_t . Clearly these topological invariants will inhibit the magnetic relaxation.

In ideal MHD, with boundary conditions (B1) or (B2), the evolution of magnetic energy – equation (9) – reduces to

$$\frac{dW}{dt} = - \int_V \mathbf{v} \cdot (\mathbf{j} \times \mathbf{B}) d^3x. \quad (25)$$

Unlike in the resistive case, if the fluid stops moving then W stops changing, because the magnetic field is frozen-in to the fluid. But the energy is also stationary if $\mathbf{j} \times \mathbf{B} = \mathbf{0}$.

Variational argument To characterise the minimum-energy state, we can use a variational argument where we treat W as a functional $W(\mathbf{B})$ and differentiate it with respect to the function $\mathbf{B}(\mathbf{x})$ using functional differentiation. The first variation of W is

$$\delta W = \frac{1}{2\mu_0} \int_V \delta(B^2) d^3x = \frac{1}{\mu_0} \int_V \mathbf{B} \cdot \delta \mathbf{B} d^3x. \quad (26)$$

If \mathbf{B} is a minimiser of W , then we must have $\delta W = 0$ for all possible perturbations $\delta \mathbf{B}$. The possible perturbations are not arbitrary: the ideal

induction equation (24) implies that they must take the form $\delta\mathbf{B} = \nabla \times (\delta\boldsymbol{\xi} \times \mathbf{B})$ for some displacement $\delta\boldsymbol{\xi}$ with $\delta\xi_n|_{\partial V} = 0$. Then

$$\delta W = \frac{1}{\mu_0} \int_V \mathbf{B} \cdot \nabla \times (\delta\boldsymbol{\xi} \times \mathbf{B}) \, d^3x \quad (27)$$

$$= - \int_V \delta\boldsymbol{\xi} \cdot (\mathbf{j} \times \mathbf{B}) \, d^3x + \frac{1}{\mu_0} \oint_{\partial V} (\delta\boldsymbol{\xi} \times \mathbf{B}) \times \mathbf{B} \cdot \hat{\mathbf{n}} \, d^2x. \quad (28)$$

The boundary term vanishes under either boundary conditions (B1) or (B2). Then $\delta W = 0$ for all perturbations $\delta\boldsymbol{\xi}$ if and only if

$$\mathbf{j} \times \mathbf{B} = \mathbf{0}. \quad (29)$$

So the minimum-energy state is a *nonlinear force-free* magnetic field of the form $\mathbf{j} = \alpha\mathbf{B}$. The coefficient α depends on \mathbf{x} but is constant along magnetic field lines (this follows from $\nabla \cdot \mathbf{j} = \nabla \cdot \mathbf{B} = 0$).

Computational methods Knowing that the relaxed state satisfies (29), how can we compute it? The need to constrain every helicity $h(V_i)$ means that an iterative method is required. Although we must ensure that the magnetic field is frozen-in to the fluid during this process, we need not follow the precise evolution given by the full MHD equations. A successful approach is to embed the magnetic field in a fictitious fluid with simplified properties, while retaining the induction equation (24). We can choose any appropriate model in which energy is dissipated and W decreases.

A simple model that achieves the required energy dissipation is to prescribe the velocity

$$\nu\mathbf{v} = \mathbf{j} \times \mathbf{B}, \quad (30)$$

instead of solving the momentum equation (2). This is called *magneto-friction* and is widely used in modelling magnetic equilibria in the Sun's corona. Substituting (30) into (25) shows that, in this model,

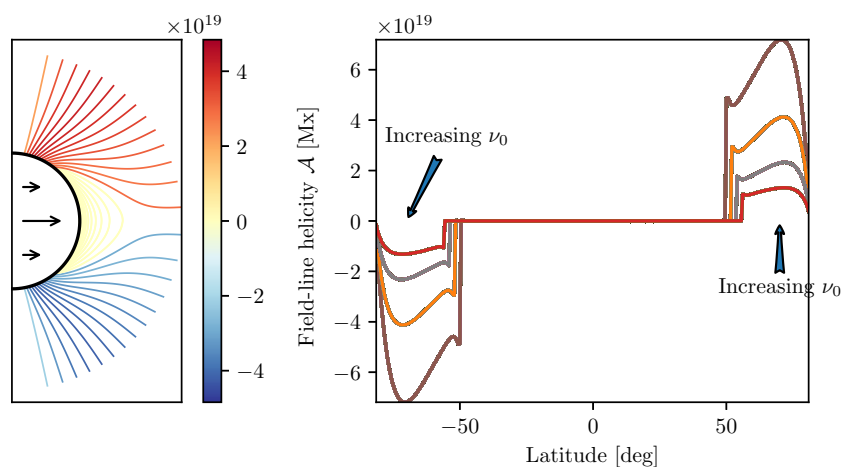
$$\frac{dW}{dt} = -\nu \int_V v^2 \, d^3x, \quad (31)$$

so that W decreases monotonically provided $\nu > 0$. Since $W \geq 0$, it must tend to a limit with $\mathbf{v} = \mathbf{0}$. By (30), this limit must satisfy $\mathbf{j} \times \mathbf{B} = \mathbf{0}$.

Magneto-friction under (30) has the disadvantage that magnetic null-points, where $\mathbf{B} = \mathbf{0}$, do not move. In addition, the relaxation will be slow at locations where B is small. To remedy the latter, the coefficient ν is usually made proportional to B , e.g. $\nu = \nu_0 B^2$ (with some correction at nulls). Since \mathbf{B} is frozen-in to the fluid, a Lagrangian numerical scheme is a natural choice (e.g. Candelaresi et al., 2015, and references therein).

Example 2.1 (Modelling the Sun’s corona). Magneto-frictional relaxation has been used in different ways as a tool for modelling force-free magnetic equilibria in the Sun’s atmosphere. One approach is to compute a single static equilibrium by enforcing a fixed vector \mathbf{B} on the solar surface (lower boundary), and evolving an initial potential state toward a force-free equilibrium through (30). This approach is exemplified by Valori et al. (2010). It requires vector magnetogram data, i.e. measurements of all three components of \mathbf{B} on the solar surface, so is presently restricted to active regions. For modelling wider regions of the solar atmosphere, an alternative approach is quasi-static: the magnetic field in the coronal volume evolves according to (30), but the boundary conditions are evolved at the same time to reflect the evolution on the real Sun. So long as the relaxation is rapid enough compared to the boundary driving, \mathbf{B} evolves quasi-statically through a continuous sequence of near force-free equilibria. In the absence of new flux emergence, a dynamical equilibrium is reached. This approach was introduced by van Ballegoijen et al. (2000), and has the advantage that free magnetic energy (and helicity) may be injected into the corona by applying surface footpoint motions, without needing to know the horizontal components of \mathbf{B} on the solar surface.

The figure below shows a dynamical equilibrium in a simple model where the Sun’s dipolar field is continually driven by rotation of the solar surface (Yeates and Hornig, 2016), while relaxing through magneto-friction.



Left: magnetic field lines in the dynamical steady state, coloured by field-line helicity \mathcal{A} (which will be discussed in Lecture 3). Right: the latitudinal

profile of \mathcal{A} for different strengths of the frictional parameter ν_0 . Larger ν_0 means slower relaxation, so the outer ends of the field lines “lag behind” their surface footpoints more, so that the open field lines support more magnetic helicity. In other words, the steady-state magnetic field is twisted. (With these parameters, this twist is too weak to be apparent in the field-line plot.) The closed field lines across the equator also lag behind, but have no net helicity by symmetry.

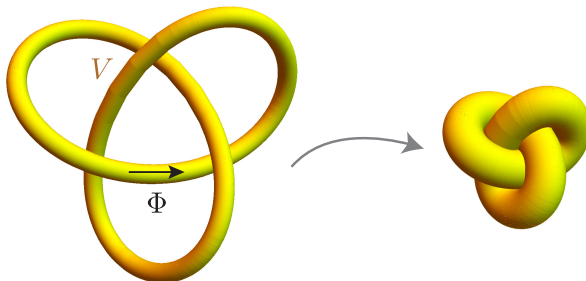
It is possible to enforce $\nabla \cdot \mathbf{v} = 0$ if we include an additional “pressure” gradient $-\nabla p$ on the right-hand side of (30) (e.g., Moffatt, 1992). The scalar function p is chosen at each time by solving the Neumann problem

$$\nabla^2 p = \nabla \cdot (\mathbf{j} \times \mathbf{B}) \quad \text{in } V, \quad (32)$$

$$\hat{\mathbf{n}} \cdot \nabla p = \hat{\mathbf{n}} \cdot (\mathbf{j} \times \mathbf{B}) \quad \text{on } \partial V. \quad (33)$$

Under this additional constraint, the resulting minimum-energy state is a magnetohydrostatic equilibrium $\mathbf{j} \times \mathbf{B} = \nabla p$.

Example 2.2 (Energy of a knot; Moffatt 1990). An interesting application of ideal magnetic relaxation is in knot theory, where one seeks “invariants” that can discriminate different knots. Moffatt (1990) proposed that the minimum, relaxed-state, magnetic energy W for a magnetic flux tube of the given knot topology could serve as such an invariant. Here is a sketch showing the relaxation of a magnetic trefoil knot to its minimum-energy configuration (after Moffatt, 1990).



Magnetic tension will tend to tighten the knot, with the flux tube expanding to conserve volume. The topology ultimately stops the relaxation.

The minimum energy will depend on the initial helicity of the tube (i.e., the amount of internal twist), which we may fix to zero. In general, there may be several different asymptotic states for the ideal relaxation, reached from different initial geometrical configurations of the knot. Moffatt (1990)

suggests that the corresponding relaxed-state energies $\{W_i\}$ define an “energy spectrum” that characterises the knot. The lowest of these energies is a measure of the knot’s complexity. For more recent work on these energies, see Ricca and Maggioni (2014).

Another way to dissipate energy in the fictitious fluid is through viscosity. For example, we can neglect the inertial and pressure terms in the momentum equation (3), so that the velocity is determined at each time by solving

$$\nabla \cdot \bar{\boldsymbol{\sigma}} = -\mathbf{j} \times \mathbf{B}. \quad (34)$$

Bajer and Moffatt (2013) use an isotropic Newtonian fluid giving the specific form

$$\mu_s \nabla^2 \mathbf{v} + \left(\frac{1}{3}\mu_s + \mu_b\right) \nabla(\nabla \cdot \mathbf{v}) = -\mathbf{j} \times \mathbf{B}. \quad (35)$$

This is more computationally expensive than magneto-friction, but avoids some of the drawbacks mentioned above. Substituting this into (25), and assuming $\mathbf{v} = \mathbf{0}$ on ∂V , shows that

$$\frac{dW}{dt} = -\mu_s \int_V \left(\frac{\partial v_i}{\partial x_j}\right)^2 d^3x - \left(\frac{1}{3}\mu_s + \mu_b\right) \int_V (\nabla \cdot \mathbf{v})^2 d^3x. \quad (36)$$

In other words, magnetic energy is again monotonically decreasing in this model. Viscous dissipation is also used in the model of Example 1.1.

2.2 Taylor Relaxation

In a seminal work, Taylor (1974) argued that the total helicity

$$H := h(V) = \int_V \mathbf{A} \cdot \mathbf{B} d^3x \quad (37)$$

will remain almost unchanged even in a resistive evolution, provided that η is small enough. Assuming that all of the other sub-helicities $h(V_t)$ would be destroyed by reconnection, he was able to predict the relaxed state under the single constraint of conserved H . Let us consider this important theory in more detail.

Approximate invariance of H Taylor’s original argument was that changes in magnetic topology under reconnection are accompanied only by very small changes in \mathbf{B} itself, so that the integrand $\mathbf{A} \cdot \mathbf{B}$ is redistributed among field lines, but not destroyed. Since H is the integral of this quantity over the whole of V , it should remain almost invariant.

This approximate invariance of H is well-supported by numerical simulations, and by a number of other theoretical arguments. To sketch some of them, we neglect boundary terms and take $V_t = V$ in equation (23) so that

$$\frac{dH}{dt} = -2 \int_V \eta \mathbf{j} \cdot \mathbf{B} \, d^3x, \quad (38)$$

and we assume purely ohmic dissipation in (9) so that

$$\frac{dW}{dt} = - \int_V \eta j^2 \, d^3x. \quad (39)$$

Some possible arguments are then:

1. *Cauchy-Schwarz inequality (Berger, 1984)*. Applying the Cauchy-Schwarz inequality (and assuming constant η) gives

$$\left| \frac{dH}{dt} \right|^2 \leq 4 \left(\int_V \eta^2 j_{\parallel}^2 \, d^3x \right) \left(\int_V B^2 \, d^3x \right) \leq 4\eta \left(\int_V \eta j^2 \, d^3x \right) (2\mu_0 W), \quad (40)$$

$$\implies \left| \frac{dH}{dt} \right| \leq \sqrt{8\mu_0 \eta W} \left| \frac{dW}{dt} \right|. \quad (41)$$

For η small, this shows that the dissipation rate of H is slower than that of W .

2. *Thinness of current sheets (Browning, 1988)*. For low η , the electric current is typically concentrated in very thin current sheets (e.g., Pontin and Hornig, 2015), so that $j \sim B/\delta$ for $\delta \ll 1$. It follows that $|\mathbf{j} \cdot \mathbf{B}| \ll j^2$, so that

$$\left| \frac{dH}{dt} \right| \ll \left| \frac{dW}{dt} \right|. \quad (42)$$

3. *Frequency spectrum (Choudhuri, 1998)*. If $V = \mathbb{R}^3$, we could take Fourier transforms

$$\mathbf{A}(\mathbf{x}) = \frac{1}{(2\pi)^{3/2}} \int_{\mathbb{R}^3} \tilde{\mathbf{A}}(\mathbf{k}) e^{i\mathbf{k} \cdot \mathbf{x}} \, d^3k, \quad (43)$$

$$\mathbf{B}(\mathbf{x}) = \frac{1}{(2\pi)^{3/2}} \int_{\mathbb{R}^3} i\mathbf{k} \times \tilde{\mathbf{A}}(\mathbf{k}) e^{i\mathbf{k} \cdot \mathbf{x}} \, d^3k, \quad (44)$$

and use $\int_{\mathbb{R}^3} e^{i(\mathbf{k}' - \mathbf{k}) \cdot \mathbf{x}} \, d^3x = (2\pi)^3 \delta(\mathbf{k}' - \mathbf{k})$ to see that

$$W = \frac{1}{2\mu_0} \int_{\mathbb{R}^3} \left| \mathbf{k} \times \tilde{\mathbf{A}}(\mathbf{k}) \right|^2 \, d^3k, \quad (45)$$

$$H = \int_{\mathbb{R}^3} i \tilde{\mathbf{A}}^*(\mathbf{k}) \cdot (\mathbf{k} \times \tilde{\mathbf{A}}(\mathbf{k})) \, d^3k. \quad (46)$$

The spectrum of H goes like $k\tilde{A}^2$ whereas that of W goes like $k^2\tilde{A}^2$. High wavenumbers therefore have a greater weight in the spectrum of W (equivalently, H has more power at larger scales). Since high-wavenumber components decay faster under ohmic diffusion, W decays faster than H .

Woltjer's theorem Having proposed that H is the only surviving constraint, Taylor invoked an earlier variational principle of Woltjer (1958) to characterise the minimum-energy state.

To impose the constraint, we introduce a constant Lagrange multiplier $\frac{1}{2}\alpha_0$ and look for \mathbf{B} such that

$$\delta(W - \frac{1}{2}\alpha_0 H) = 0. \quad (47)$$

The perturbations must obey $\nabla \cdot \delta\mathbf{B} = 0$, and this means that we can write $\delta\mathbf{B} = \nabla \times \delta\mathbf{A}$. The choice of $\delta\mathbf{A}$ is not unique, but since $B_n|_{\partial V}$ remains unchanged under either boundary conditions (B1) or (B2), we can choose a gauge where $\delta\mathbf{A} \times \hat{\mathbf{n}}|_{\partial V} = 0$. Then

$$\delta W = \frac{1}{\mu_0} \int_V \mathbf{B} \cdot \nabla \times \delta\mathbf{A} \, d^3x, \quad (48)$$

$$= \frac{1}{\mu_0} \int_V (\delta\mathbf{A} \cdot \nabla \times \mathbf{B} - \nabla \cdot [\mathbf{B} \times \delta\mathbf{A}]) \, d^3x, \quad (49)$$

$$= \int_V \delta\mathbf{A} \cdot \mathbf{j} \, d^3x - \frac{1}{\mu_0} \oint_{\partial V} \mathbf{B} \cdot (\delta\mathbf{A} \times \hat{\mathbf{n}}) \, d^2x, \quad (50)$$

$$= \int_V \delta\mathbf{A} \cdot \mathbf{j} \, d^3x. \quad (51)$$

We then calculate

$$\delta H = \int_V \delta\mathbf{A} \cdot \mathbf{B} \, d^3x + \int_V \mathbf{A} \cdot \delta\mathbf{B} \, d^3x \quad (52)$$

$$= \int_V \delta\mathbf{A} \cdot \mathbf{B} \, d^3x + \int_V \mathbf{A} \cdot \nabla \times \delta\mathbf{A} \, d^3x \quad (53)$$

$$= \int_V \delta\mathbf{A} \cdot \mathbf{B} \, d^3x + \int_V \delta\mathbf{A} \cdot \nabla \times \mathbf{A} \, d^3x - \oint_{\partial V} \hat{\mathbf{n}} \cdot (\mathbf{A} \times \delta\mathbf{A}) \, d^2x \quad (54)$$

$$= 2 \int_V \delta\mathbf{A} \cdot \mathbf{B} \, d^3x - \oint_{\partial V} \mathbf{A} \cdot (\delta\mathbf{A} \times \hat{\mathbf{n}}) \, d^2x \quad (55)$$

$$= 2 \int_V \delta\mathbf{A} \cdot \mathbf{B} \, d^3x, \quad (56)$$

where we again used the gauge condition in the final step. Combining (51) and (56), we see that a minimum-energy state must satisfy

$$\int_V \delta \mathbf{A} \cdot (\mathbf{j} - \alpha_0 \mathbf{B}) \, d^3x = 0, \quad (57)$$

and if this is true for all perturbations then

$$\mathbf{j} = \alpha_0 \mathbf{B}. \quad (58)$$

This is a *linear force-free field*, since α_0 is constant.

Some remarks:

1. Woltjer's original paper (Woltjer, 1958) made the more restrictive assumption that $\delta \mathbf{A}|_{\partial V} = \mathbf{0}$.
2. Since $\mu_0 \mathbf{j} = \nabla \times \mathbf{B}$, equation (58) may be interpreted as an eigenvalue equation for the curl operator, with eigenvalues $\mu_0 \alpha_0$ and corresponding eigenstates \mathbf{B} (e.g. Cantarella et al., 2000).
3. The above variational principle is purely "formal," but Laurence and Avellaneda (1991) later put it on a more rigorous footing by proving that the minimiser is attained and satisfies (58).

In general there may be multiple possible solutions to (58) for a discrete set of possible "eigenvalues" α_0 . The minimum-energy state will be the one with smallest W .

Example 2.3 (Periodic cylinder; Taylor 1974, 1986; Biskamp 1997). Taylor's original application of his theory was to the minimum-energy state of a plasma in a periodic cylinder, representing a toroidal fusion device.

Let the cylinder have length $2\pi d$ and radius R , and impose periodic boundary conditions $\mathbf{B}(r, \phi, \pi d) = \mathbf{B}(r, \phi, -\pi d)$. Separation of variables shows that the general solution to (58) in such a domain has the form $\mathbf{B} = \sum_{m,k \in \mathbb{Z}} c_{m,k} \mathbf{B}^{m,k}$, where

$$B_r^{m,k} = - \left[\frac{k}{q} J'_m(qr) + \frac{m\alpha_0}{rq^2} J_m(qr) \right] \sin(m\phi + kz), \quad (59)$$

$$B_\phi^{m,k} = - \left[\frac{\alpha_0}{q} J'_m(qr) + \frac{mk}{rq^2} J_m(qr) \right] \cos(m\phi + kz), \quad (60)$$

$$B_z^{m,k} = J_m(qr) \cos(m\phi + kz), \quad (61)$$

and $q = \sqrt{\alpha_0^2 - k^2}$. The functions J_m are Bessel functions of the first kind. Our task is to find the specific solution with minimum energy for a given helicity H and a given "toroidal" flux $\Phi = \int_{z=\text{const.}} B_z \, dS$. Since H is gauge dependent here, it is customary to fix a specific H by choosing

a vector potential satisfying $\int_{-\pi d}^{\pi d} A_z(R, \phi, z) dz = 0$ on the side boundary (topologically, this means that \widehat{H} is not measuring linkage with magnetic flux outside the cylinder). Thus we take

$$\mathbf{A} = \frac{1}{\alpha_0} \left(\mathbf{B} - c_{0,0} J_0(\alpha_0 R) \hat{\mathbf{z}} \right). \quad (62)$$

1. *Axisymmetric solution* ($m = k = 0$). This exists for any value of α_0 , with $\mathbf{B} = c_{0,0} [J_1(\alpha_0 r) \hat{\boldsymbol{\phi}} + J_0(\alpha_0 r) \hat{\mathbf{z}}]$. The constants $c_{0,0}$ and α_0 must be fixed by Φ and the initial helicity H . Firstly,

$$\Phi = 2\pi c_{0,0} \int_0^R J_0(\alpha_0 r) r dr = \frac{2\pi R c_{0,0}}{\alpha_0} J_1(\alpha_0 R). \quad (63)$$

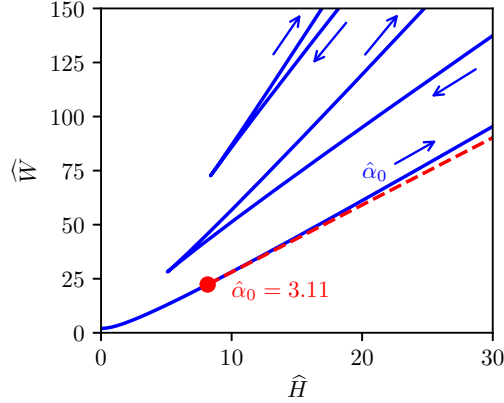
After some calculation, we find that the normalised helicity $\widehat{H} = RH/(d\Phi^2)$ satisfies

$$\widehat{H} = \hat{\alpha}_0 \left(1 + \frac{J_0^2(\hat{\alpha}_0)}{J_1^2(\hat{\alpha}_0)} \right) - 2 \frac{J_0(\hat{\alpha}_0)}{J_1(\hat{\alpha}_0)}, \quad (64)$$

where $\hat{\alpha}_0 = \alpha_0 R$. In fact, there are multiple solutions for different $\hat{\alpha}_0$ having the same \widehat{H} . The minimum-energy solution we seek is the one with lowest energy. The normalised energy $\widehat{W} = 2R^2 \mu_0 W/(d\Phi^2)$ is given by

$$\widehat{W} = \hat{\alpha}_0^2 \left(1 + \frac{J_0^2(\hat{\alpha}_0)}{J_1^2(\hat{\alpha}_0)} \right) - \hat{\alpha}_0 \frac{J_0(\hat{\alpha}_0)}{J_1(\hat{\alpha}_0)}, \quad (65)$$

so that equations (64) and (65) generate a parametric plot of $\widehat{W}(\widehat{H})$ as $\hat{\alpha}_0$ varies, shown by the blue solid curves below:



Each solution branch corresponds to values of $\hat{\alpha}_0$ between two zeros of J_1 . The lowest energy branch is that with $\hat{\alpha}_0 < 3.83$ (first non-zero root of J_1).

2. *Helical solutions.* It turns out that the minimum-energy solution is axisymmetric only if $\hat{\alpha}_0 < 3.11$ (corresponding to $\hat{H} = 8.21$). For larger $\hat{\alpha}_0$, a superposition of the axisymmetric solution and an $m = 1$ mode has lower energy. This is indicated by the red dashed line in the plot above. (This curve is different to those for the axisymmetric mode in that the whole curve corresponds to a fixed value $\hat{\alpha}_0 = 3.11$. As \hat{H} varies, it is the constant $c_{1,0}$ that changes.) For more details, see Reiman (1980).

Because the $m = k = 0$ solution can reproduce sign reversals in B_z , Taylor's hypothesis was successful in explaining this feature of the reversed-field pinch device, and was subsequently applied to model relaxed states in other systems such as the solar atmosphere. However, it is not clear that H is the only constraint in many systems.

3 Field-Line Helicity in Relaxation

In this final lecture, we revisit Taylor's argument (Section 2.2) that the integrand $\mathbf{A} \cdot \mathbf{B}$ will be redistributed among magnetic field lines, rather than destroyed. This implies not only that the total helicity H is conserved, but that the distribution of values of $\mathbf{A} \cdot \mathbf{B}$ is also conserved, albeit exchanged between field lines. If that distribution does not match that of the Woltjer minimum-energy state, this suggests that such a state can not be reached.

To address this quantitatively, we will avoid talking about the density $\mathbf{A} \cdot \mathbf{B}$, which is not invariant under an ideal evolution¹. Rather, we consider the individual ideal invariants $h(V_t)$ for magnetically-closed subvolumes V_t .

3.1 Field-line helicity

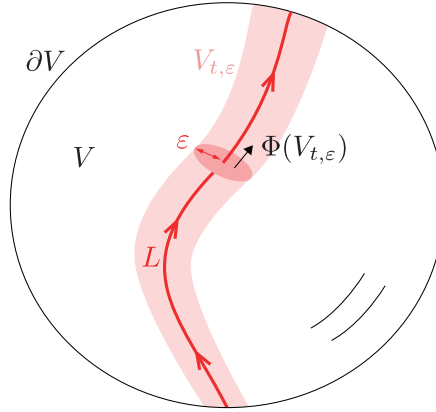
The finest possible decomposition of V into disjoint magnetically-closed subvolumes V_t is to consider infinitesimally thin tubes around individual magnetic field lines. This approach is most useful when there are multiple different magnetic field lines in V ; if a single ergodic field line fills V , then there will be only a single subvolume. Since $h(V_t)$ is a volume integral, we

¹Whilst you can make $\mathbf{A} \cdot \mathbf{B}$ into a material scalar by choosing an appropriate gauge (Webb et al., 2010), this would remove the utility of field-line helicity as a measure of changes in magnetic topology. Instead, a gauge of \mathbf{A} should be chosen that is fixed in time (at least on the boundaries where it affects the $h(V_t)$).

will normalize to get a finite value, and define

$$\mathcal{A}(L) = \lim_{\varepsilon \rightarrow 0} \frac{h(V_{t,\varepsilon})}{\Phi(V_{t,\varepsilon})}, \quad (66)$$

where $V_{t,\varepsilon}$ is a tubular magnetic flux tube traced from some circle of radius ε in a fixed cross-sectional surface. In the limit $\varepsilon \rightarrow 0$, the tube $V_{t,\varepsilon}$ collapses to the line L , and $\mathcal{A}(L)$ tends to a well-defined limit – independent of the choice of cross section – called the *field-line helicity* of L (Berger, 1988). The geometry is sketched below; here L intersects ∂V at both ends:



Equation (66) shows that \mathcal{A} has the dimensions of a magnetic flux. From the definition of $h(V_t)$, it follows that

$$\mathcal{A}(L) = \int_L \mathbf{A} \cdot d\mathbf{l}, \quad (67)$$

so when L is a closed loop $\mathcal{A}(L)$ is simply the magnetic flux linked through that loop. When L is not a closed loop, the topological interpretation of $\mathcal{A}(L)$ is more nuanced, and – like the value of $\mathcal{A}(L)$ – depends on the chosen gauge of \mathbf{A} . However, it still represents, in some general sense, the magnetic flux linked with L . It is a topological invariant in ideal MHD, just like $h(V_t)$. We can recover the total helicity H if we integrate $\mathcal{A}(L)$ over all field lines, weighted by infinitesimal magnetic flux.

Visualisation is simplest if \mathbf{B} has a global cross-sectional surface, through which all magnetic field lines pass. If field line L intersects S at (x_1, x_2) , then we can write

$$H = \int_S \mathcal{A}(L(x_1, x_2)) B_n(x_1, x_2) d^2x \quad (68)$$

and we can plot the distribution of \mathcal{A} on the surface S . This will be used in Example 3.1 later.

Ideal invariance Consider the ideal-MHD evolution of field-line helicity $\mathcal{A}(L)$ for some magnetic field line L . In an ideal evolution with \mathbf{B} frozen to the fluid, L will be a material line, and each $V_{t,\varepsilon}$ will be a material volume with invariant flux $\Phi(V_{t,\varepsilon})$. The behaviour of $\mathcal{A}(L)$ thus depends only on $h(V_{t,\varepsilon})$. For $\eta = 0$, equation (23) reduces to a boundary integral and

$$\frac{d\mathcal{A}(L)}{dt} = \lim_{\varepsilon \rightarrow 0} \frac{1}{\Phi(V_{t,\varepsilon})} \oint_{\partial V_{t,\varepsilon}} (\chi + \mathbf{v} \cdot \mathbf{A}) B_n d^2x. \quad (69)$$

This integral will clearly vanish if L is a closed curve (provided χ is single-valued). This is expected since, in that case, $\mathcal{A}(L)$ is gauge invariant and by (67) is precisely the magnetic flux linked through L .

The integral can also be made to vanish in more general situations by fixing an appropriate gauge of \mathbf{A} , which is equivalent to choosing the potential χ . For example, suppose the field line L is rooted at both ends on the domain boundary ∂V where condition (B2) holds. Since $\partial B_n / \partial t = 0$ on ∂V , we can keep $\chi = 0$ there, which essentially corresponds to keeping the gauge of \mathbf{A} fixed in time on the ∂V boundary. In that case, we again have

$$\frac{d\mathcal{A}(L)}{dt} = 0, \quad (70)$$

since $\mathbf{v} = \mathbf{0}$ on the ends of $V_{t,\varepsilon}$ and $B_n = 0$ on the side boundaries of $V_{t,\varepsilon}$ (which is a magnetic flux tube).

3.2 Resistive evolution in a non-null magnetic field

To make sense of $d\mathcal{A}(L)/dt$ in a non-ideal evolution ($\eta \neq 0$), we must first specify how to identify a field line L from one time to the next, since field lines are no longer material lines.

We will simplify the problem by assuming that all field lines are rooted in an ideal boundary where we impose $\eta \mathbf{j}|_{\partial V} = \mathbf{0}$ in addition to boundary conditions (B2). We identify each field line L at each time by fixing its startpoint in the $B_n < 0$ region of ∂V (which we denote ∂V^-). The corresponding endpoints would be stationary in ideal MHD, but can move around on ∂V in a non-ideal evolution.

Since L is no longer a material line, $V_{t,\varepsilon}$ need no longer be a material volume, $\Phi(V_{t,\varepsilon})$ need no longer be invariant, and furthermore we can no longer apply (23). However, if we assume that $\mathbf{B} \neq \mathbf{0}$, so that there are no null points in our magnetic field, then we can make progress.

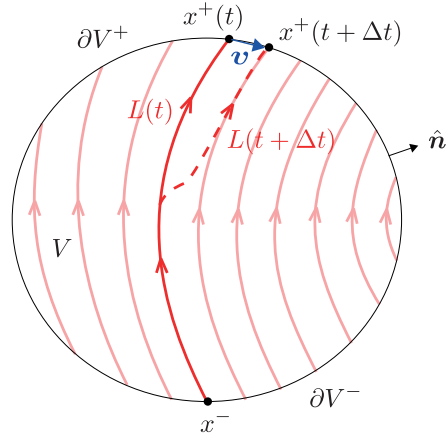
The advantage of having $\mathbf{B} \neq \mathbf{0}$ is that we can globally decompose $\eta\mathbf{j}$ into components parallel and perpendicular to \mathbf{B} , writing it in the form

$$\eta\mathbf{j} = -\mathbf{u} \times \mathbf{B} + \nabla\psi. \quad (71)$$

In that case, the induction equation (6) becomes

$$\frac{\partial\mathbf{B}}{\partial t} = \nabla \times [(\mathbf{v} + \mathbf{u}) \times \mathbf{B}], \quad (72)$$

showing that the magnetic field is frozen-in to the flow of a *field-line velocity* $\mathbf{v} + \mathbf{u}$ that differs from the fluid velocity \mathbf{v} by a slipping velocity \mathbf{u} . Since $\mathbf{j} = \mathbf{0}$, we may choose $\mathbf{u}|_{\partial V^-} = \mathbf{0}$, so that we are following field lines traced from a fixed point on ∂V^- . But (71) implies that we will generally have $\mathbf{u}|_{\partial V^+} \neq \mathbf{0}$ because $\nabla\psi \neq \mathbf{0}$ on ∂V^+ . The situation is sketched below:



If there were a null point where $\mathbf{B} = \mathbf{0}$, then the decomposition (71) would break down at the null where the perpendicular and parallel directions are not defined. Correspondingly, there would be no global field line velocity $\mathbf{v} + \mathbf{u}$, allowing field lines to break discontinuously at the null.

Since \mathbf{B} is frozen-in to the effective flow $\mathbf{v} + \mathbf{u}$, the flux tube $V_{t,\varepsilon}$ will be a material volume with respect to this flow. This means that it will have invariant flux $\Phi(V_{t,\varepsilon})$. Moreover, we may use the transport theorem, as we did in Lecture 1, to show that

$$\frac{d\mathcal{A}(L)}{dt} = \lim_{\varepsilon \rightarrow 0} \frac{1}{\Phi(V_{t,\varepsilon})} \oint_{\partial V_t} [\chi - \psi + (\mathbf{v} + \mathbf{u}) \cdot \mathbf{A}] B_n d^2x \quad (73)$$

for some scalar potential χ . This looks very similar to the ideal case, except for the additional potential ψ (non-zero only in ∂V^+) and the additional slipping velocity \mathbf{u} .

In principle, we could make $\mathcal{A}(L)$ invariant by setting $\chi = \psi - (\mathbf{v} + \mathbf{u}) \cdot \mathbf{A}$. However, the gauge of \mathbf{A} on ∂V would then be time-dependent, so that we would be removing any information contained in the evolution of \mathcal{A} .

Instead, it is more informative to fix the gauge χ over time, so let us set $\chi = 0$ (for simplicity). Since ψ , \mathbf{v} and \mathbf{u} vanish on ∂V_- , and we have $\mathbf{v} = \mathbf{0}$ on ∂V , this leaves the evolution equation

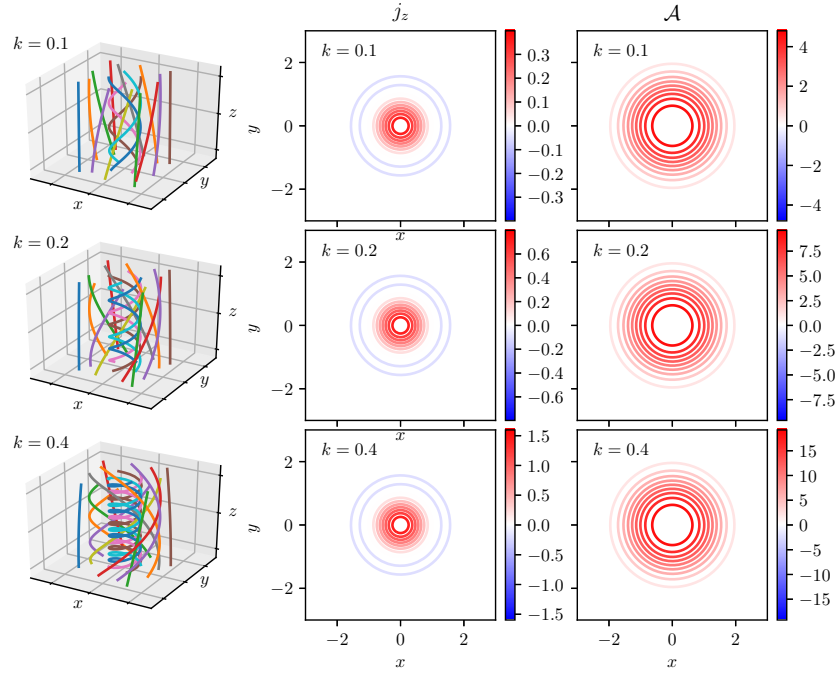
$$\begin{aligned} \frac{d\mathcal{A}(L)}{dt} &= \lim_{\varepsilon \rightarrow 0} \frac{1}{\Phi(V_{t,\varepsilon})} \oint_{\partial V_t \cap \partial V^+} (\mathbf{u} \cdot \mathbf{A} - \psi) B_n d^2x \\ &= (\mathbf{u} \cdot \mathbf{A} - \psi) \Big|_{x^+(t)}, \end{aligned} \quad (74)$$

where $x^+(t)$ is the endpoint of L on ∂V^+ , \mathbf{u} is the slipping velocity, and $\psi = \int_L \eta \mathbf{j} \cdot d\mathbf{l}$. To recap, this expression holds for a field line L traced from an ideal boundary in a non-null magnetic field.

Example 3.1 (Reconnection in a twisted magnetic field). During a resistive relaxation, \mathcal{A} will change due to magnetic reconnection. In this example, we consider the effect of a single local reconnection site in a wider magnetic field. In cylindrical coordinates (r, ϕ, z) , the initial magnetic field has the axisymmetric form $\mathbf{B} = \nabla \times \mathbf{A}$ where $\mathbf{A} = (r/2)\hat{\phi} + f(r)\hat{z}$ and $f(r) = k e^{-r^2}$. The current density is purely axial, $\mu_0 \mathbf{j} = 4k(1 - r^2) e^{-r^2} \hat{z}$. Since the field lines lie on cylindrical surfaces, it is straightforward to compute the field-line helicity in this gauge, giving

$$\mathcal{A}(r) = 2dk(1 + r^2) e^{-r^2}, \quad (75)$$

where $2d$ is the length of the domain in z . The figure below shows this magnetic field for three values of the ‘‘twist’’ parameter k . Colour scales for j_z and \mathcal{A} are capped at \pm maximum absolute value, and the three-dimensional plots are compressed in the z direction for clarity.



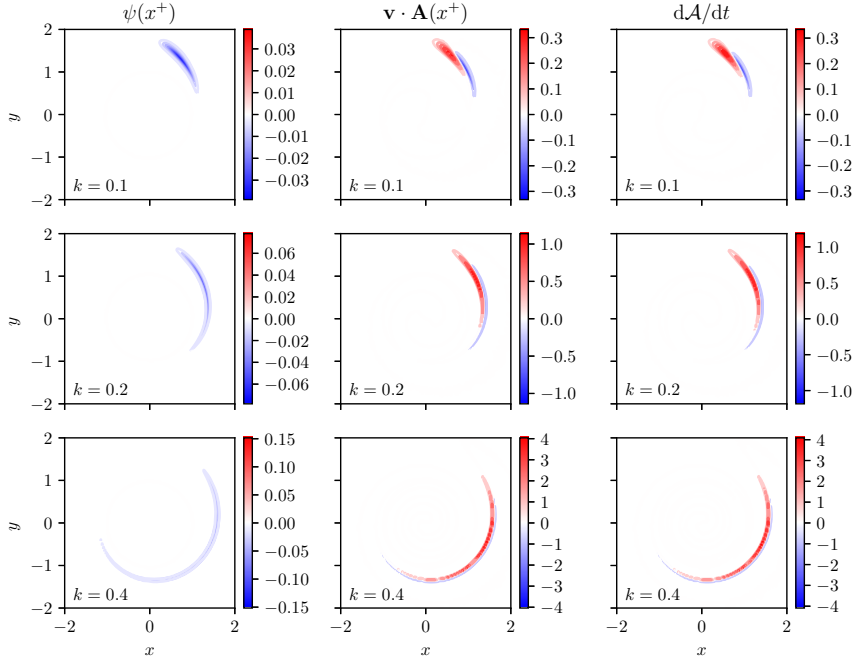
Let us now consider how this would evolve under the influence of a single localised reconnection site. In a real magnetic field, localised reconnection would arise from localisation of j in a sharp current sheet. However, we can model the basic effect by instead localising the resistivity with a gaussian form

$$\eta(x, y, z) = \exp\left(-\frac{x^2 + (y - y_0)^2 + z^2}{(\frac{1}{5})^2}\right), \quad (76)$$

describing a spherical “diffusion region” of radius $\frac{1}{5}$ and centred at $(0, y_0, 0)$ (displaced from the symmetry axis). Neglecting fluid velocity, we then consider how \mathcal{A} changes under pure diffusion,

$$\frac{\partial \mathcal{A}}{\partial t} = -\nabla \times (\eta \mathbf{j}). \quad (77)$$

The figure below shows the terms in equation (74), for our three values of k . Again, colour scales are capped at \pm maximum absolute value.



Here, we have computed $\psi(x^+)$ by integrating $\eta \mathbf{j}$ along magnetic field lines traced from a grid of starting points x^- . The slipping velocity \mathbf{u} at each end-point $x^+ \in \partial V^+$ has been computed by first estimating $\nabla \psi$ at x^+ using finite differences (which requires integrating ψ along several field lines ending near x^+), then using

$$\mathbf{u} = \frac{\mathbf{z} \times \nabla \psi}{B_z}. \quad (78)$$

This may be derived from (71) if we choose $u_z \equiv 0$ and use the fact that $\eta \mathbf{j}$ vanishes on the boundary ∂V^+ . Choosing $u_z \equiv 0$ is possible because we can always add an arbitrary component of \mathbf{u} parallel to \mathbf{B} without changing $\mathbf{u} \times \mathbf{B}$. With $u_z \equiv 0$ we ensure that the computed change in \mathcal{A} matches what would be found by integrating \mathbf{A} only between the boundaries $z = -d$ and $z = d$.

Several observations are apparent from the figures above:

1. The terms are non-zero only for those field lines that pass through the diffusion region, reflecting the fact that ideal evolution does not change \mathcal{A} (since the field-line end-points are fixed). The corresponding footprint regions become more stretched out as k increases.

2. The change in \mathcal{A} is dominated by the $\mathbf{u} \cdot \mathbf{A}$ term, with the contribution from ψ an order of magnitude smaller. The difference between $\mathbf{u} \cdot \mathbf{A}$ and ψ increases for larger k , with $\|\mathbf{u} \cdot \mathbf{A}\|_\infty \sim k^2$ (so that $\|\mathrm{d}\mathcal{A}/\mathrm{d}t\|_\infty \sim k^2$) but $\|\psi\|_\infty \sim k$.
 3. The distribution of $\mathrm{d}\mathcal{A}/\mathrm{d}t$ tends to have approximately equal positive and negative regions, so that the overall net change is much smaller than the maximum local change. For example, with $k = 0.4$ we have $\int_{\partial V^-} \mathrm{d}\mathcal{A}/\mathrm{d}t \, \mathrm{d}^2x \approx 4 \times 10^{-2}$, but $\int_{\partial V^-} |\mathrm{d}\mathcal{A}/\mathrm{d}t| \, \mathrm{d}^2x \approx 7 \times 10^{-1}$.
-

3.3 Consequences for relaxation theory

The observations in Example 3.1 turn out to be rather general properties that apply to MHD relaxation in any non-null magnetic field with sufficiently complex field-line structure (Russell et al., 2015). Although we have considered a simple axisymmetric field, it is even easier to obtain the required complexity in a fully three-dimensional, turbulent system. To finish, we will explain why this behaviour arises.

Dominance of $\mathbf{u} \cdot \mathbf{A}$ term A simple scaling analysis shows why the complexity of the field-line structure matters. Let Δ be the scale on which \mathbf{B} varies, then $A \sim \Delta B$. To see how \mathbf{u} scales, we use (78) to see that $u \sim |\nabla\psi|/B$. In $\nabla\psi$ we are taking the gradient of a field-line integrated quantity, which changes on the scale of gradients in the field-line mapping. Due to the stretching evident in Example 3.1, this is a smaller scale, δ . Thus

$$|\mathbf{u} \cdot \mathbf{A}| \sim \frac{|\psi|}{\delta B} \Delta B = \frac{\Delta}{\delta} |\psi|. \quad (79)$$

So long as we have a scale separation Δ/δ , this explains why the evolution of \mathcal{A} is dominated by the $\mathbf{u} \cdot \mathbf{A}$ term.

Redistribution rather than dissipation The fact that

$$\left| \int_{\partial V^-} \frac{\mathrm{d}\mathcal{A}}{\mathrm{d}t} \, \mathrm{d}^2x \right| \ll \int_{\partial V^-} \left| \frac{\mathrm{d}\mathcal{A}}{\mathrm{d}t} \right| \, \mathrm{d}^2x \quad (80)$$

arises because of the fact that the slipping motion \mathbf{u} is along contours of ψ on ∂V^+ . Since these contours are stretched into very thin shapes (with width δ), points with oppositely directed slipping motions are in close proximity to one another. Since \mathbf{A} changes on the larger scale Δ , the product $\mathbf{u} \cdot \mathbf{A}$ changes sign with the direction of \mathbf{u} , leading to patches of opposite sign like those in Example 3.1.

Inequality (80) is a significant conclusion: it shows that field-line helicity will preferentially be redistributed during reconnection, rather than destroyed. If the scale δ is small, this redistribution can be very rapid. Thus we arrive at a refined version of Taylor’s hypothesis – in addition to conserving total helicity H , we expect that *in sufficiently complex magnetic fields, reconnection will tend to redistribute field-line helicity between field lines, rather than destroying it.*

4 Further Reading

Inevitably, a large amount of the existing literature has been omitted. This final section provides some selected pointers to other work.

Pressure and density A significant omission from the relaxation theories in Lectures 2 and 3 is the effect of the fluid pressure, p . Unlike a force-free field with $\mathbf{j} \times \mathbf{B} = 0$, a magnetohydrostatic equilibrium,

$$\mathbf{j} \times \mathbf{B} = \nabla p, \tag{81}$$

allows for a localised magnetic field by providing a confining force ∇p . This is illustrated by Smiet et al. (2017), who used ideal magnetic relaxation (with a Lagrangian code) to produce localised magnetohydrostatic equilibria having the topology of the so-called Hopf field. Their final states have significant ∇p , even though p was initially uniform.

Computing equilibria of the form (81) directly is difficult in the three-dimensional case, owing to the possibility of stochastic/ergodic regions. In such regions, filled by a single magnetic field line, pressure must be constant since (81) implies that $\mathbf{B} \cdot \nabla p = 0$. But toroidal equilibria also have an infinite number of toroidal flux surfaces, on which ∇p is non-zero. The pressure p will therefore be a rather complex function of space. The widely-used numerical code VMEC for solving (81) (Hirshman and Whitson, 1983) precludes stochastic regions by assuming a nested family of flux surfaces, but more sophisticated models with “stepped-pressure equilibria” are under development (Hudson et al., 2012).

Even if the fluid pressure is negligible, Bajer and Moffatt (2013) show that we expect significant density variations to be generated by the magnetic relaxation process. These arise because the system naturally pushes fluid in towards magnetic null points, in order to try and equalise magnetic pressure. In this way, the dynamical phase of the relaxation is expected to leave a lasting imprint in the fluid itself.

Extending Taylor theory The idea of adding additional constraints to Taylor’s basic hypothesis of conserved H is not new. This has been motivated, for example, by measurements of spatially varying α in fusion devices, where the toroidal current is often smaller nearer to the vessel wall. Regarding additional constraints, Bhattacharjee and Dewar (1982) argue that, since the individual subvolume helicities $h(V_i)$ are not conserved, one ought to instead retain additional *global* ideal constraints. They consider magnetic fields $\mathbf{B} = (\nabla\zeta - \Phi'(\Psi)\nabla\theta) \times \nabla\Psi$ that lie on toroidal flux surfaces, where Ψ and Φ denote toroidal and poloidal magnetic flux functions, respectively. Given any chosen set of ideal constraints $\{K[\omega_i]\}$ of the form

$$K[\omega_i] = \frac{1}{2} \int_V \omega_i(\Psi, \Phi) \mathbf{A} \cdot \mathbf{B} \, d^3x, \quad (82)$$

with each ω_i some chosen function, they show that the corresponding minimum-energy states must be nonlinear force-free fields of the form

$$\mathbf{j} = \sum_i \alpha_i \left(\frac{\Psi}{2} \frac{\partial \omega_i}{\partial \Psi} + \frac{\Phi}{2} \frac{\partial \omega_i}{\partial \Phi} + \omega_i \right) \mathbf{B}. \quad (83)$$

The single constraint $\omega_i = 2$ is equivalent to standard Taylor theory. The case with two constraints $\omega_1(\Psi, \Phi) = 2$ and $\omega_2(\Psi, \Phi) = (q_s\Psi + \Phi)^2$ was proposed as a better model for laboratory plasmas whose relaxed states are dominated by a single helical tearing mode. The constant q_s is set to the pitch of the desired dominant mode, so that the constraint $K[\omega_2]$ effectively enforces invariance of the helicity of that particular mode. The theory does not predict which mode will be dominant, so this needs to be established some other way (e.g., Paccagnella, 2016).

Recent MHD simulations of braided solar coronal loops have found that the relaxation process is poorly modelled by Taylor’s theory (Pontin et al., 2016), and that the final state is a nonlinear rather than linear force-free field (motivating, indeed, the work in Lecture 3). However, even applying the original Taylor theory in astrophysical systems like the Sun’s corona has its own complications. One issue is that the domain V where relaxation occurs does not have a definite fixed boundary. Rather, it has a free boundary that may expand during the relaxation process itself (e.g., Bareford et al., 2013), and which is not predicted by the Taylor theory. Globally, the classic picture of Heyvaerts and Priest (1984) envisages dividing the corona into individual magnetic flux tubes (“coronal loops”) in which localised relaxation events occur independently. However, recent work by Hussain et al. (2017) used Taylor theory to approximate the energy released in an MHD simulation of an “avalanche” of relaxation events in neighbouring coronal loops – here

the instability of one loop triggers that of a neighbour, in a chain reaction. In this merging application, the radius of each subsequent merged loop was determined by equating internal and external magnetic pressure. Finally, we note that free boundaries are not limited to astrophysics: Gimblett et al. (2006) have developed a model for Taylor relaxation in the outer region of a tokamak plasma that predicts the energy losses due to an edge-localised mode.

Bibliography

- K. Bajer and H. K. Moffatt. Magnetic Relaxation, Current Sheets, and Structure Formation in an Extremely Tenuous Fluid Medium. *Astrophys. J.*, 779:169, December 2013. doi: 10.1088/0004-637X/779/2/169.
- M. R. Bareford, A. W. Hood, and P. K. Browning. Coronal heating by the partial relaxation of twisted loops. *Astron. Astrophys.*, 550:A40, February 2013. doi: 10.1051/0004-6361/201219725.
- M. A. Berger. Rigorous new limits on magnetic helicity dissipation in the solar corona. *Geophysical and Astrophysical Fluid Dynamics*, 30:79–104, September 1984. doi: 10.1080/03091928408210078.
- M. A. Berger. An energy formula for nonlinear force-free magnetic fields. *Astron. Astrophys.*, 201:355–361, August 1988.
- A. Bhattacharjee and R. L. Dewar. Energy principle with global invariants. *Phys.Fluids*, 25:887–897, May 1982. doi: 10.1063/1.863819.
- D. Biskamp. *Nonlinear Magnetohydrodynamics*. July 1997.
- P. K. Browning. Helicity injection and relaxation in a solar-coronal magnetic loop with a free surface. *J. Plasma Phys.*, 40:263–280, October 1988. doi: 10.1017/S002237780001326X.
- S. Candelaresi, D. I. Pontin, and G. Hornig. Magnetic Field Relaxation and Current Sheets in an Ideal Plasma. *Astrophys. J.*, 808:134, August 2015. doi: 10.1088/0004-637X/808/2/134.
- J. Cantarella, D. DeTurck, H. Gluck, and M. Teytel. The spectrum of the curl operator on spherically symmetric domains. *Physics of Plasmas*, 7: 2766–2775, July 2000. doi: 10.1063/1.874127.
- A. R. Choudhuri. *The physics of fluids and plasmas : an introduction for astrophysicists* /. November 1998.
- C. G. Gimblett, R. J. Hastie, and P. Helander. Model for Current-Driven Edge-Localized Modes. *Phys. Rev. Lett.*, 96(3):035006, January 2006. doi: 10.1103/PhysRevLett.96.035006.
- J. Heyvaerts and E. R. Priest. Coronal heating by reconnection in DC current systems - A theory based on Taylor’s hypothesis. *Astron. Astrophys.*, 137:63–78, August 1984.

- S. P. Hirshman and J. C. Whitson. Steepest-descent moment method for three-dimensional magnetohydrodynamic equilibria. *Phys. Fluids*, 26: 3553–3568, December 1983. doi: 10.1063/1.864116.
- S. R. Hudson, R. L. Dewar, G. Dennis, M. J. Hole, M. McGann, G. von Nessi, and S. Lazerson. Computation of multi-region relaxed magnetohydrodynamic equilibria. *Phys. Plasmas*, 19(11):112502, November 2012. doi: 10.1063/1.4765691.
- A. S. Hussain, P. K. Browning, and A. W. Hood. A relaxation model of coronal heating in multiple interacting flux ropes. *Astron. Astrophys.*, 600:A5, April 2017. doi: 10.1051/0004-6361/201629589.
- P. Laurence and M. Avellaneda. On Woltjer’s variational principle for force-free fields. *Journal of Mathematical Physics*, 32:1240–1253, May 1991. doi: 10.1063/1.529321.
- H. K. Moffatt. The energy spectrum of knots and links. *Nature*, 347:367–369, September 1990. doi: 10.1038/347367a0.
- H. K. Moffatt. Relaxation under topological constraints. In H. K. Moffatt, G. M. Zaslavsky, P. Comte, and M. Tabor, editors, *Topological Aspects of the Dynamics of Fluids and Plasmas*, pages 3–28. Springer Netherlands, Dordrecht, 1992.
- H. K. Moffatt. Magnetic relaxation and the Taylor conjecture. *J. Plasma Phys.*, 81(6):905810608, December 2015. doi: 10.1017/S0022377815001269.
- R. Paccagnella. Relaxation models for single helical reversed field pinch plasmas. *Phys. Plasmas*, 23(9):092512, September 2016. doi: 10.1063/1.4963677.
- D. I. Pontin and G. Hornig. The Structure of Current Layers and Degree of Field-line Braiding in Coronal Loops. *Astrophys. J.*, 805:47, May 2015. doi: 10.1088/0004-637X/805/1/47.
- D. I. Pontin, S. Candelaresi, A. J. B. Russell, and G. Hornig. Braided magnetic fields: equilibria, relaxation and heating. *Plasma Phys. Contr. Fusion*, 58(5):054008, May 2016. doi: 10.1088/0741-3335/58/5/054008.
- A. Reiman. Minimum energy state of a toroidal discharge. *Phys. Fluids*, 23:230–231, January 1980. doi: 10.1063/1.862857.
- R. L. Ricca and F. Maggioni. On the groundstate energy spectrum of magnetic knots and links. *J. Phys. A Math. General*, 47(20):205501, May 2014. doi: 10.1088/1751-8113/47/20/205501.
- A. J. B. Russell, A. R. Yeates, G. Hornig, and A. L. Wilmot-Smith. Evolution of field line helicity during magnetic reconnection. *Phys. Plasmas*, 22(3):032106, March 2015. doi: 10.1063/1.4913489.
- C. B. Smiet, S. Candelaresi, and D. Bouwmeester. Ideal relaxation of the Hopf fibration. *Phys. Plasmas*, 24(7):072110, July 2017. doi: 10.1063/1.4990076.

- J. B. Taylor. Relaxation of Toroidal Plasma and Generation of Reverse Magnetic Fields. *Physical Review Letters*, 33:1139–1141, November 1974. doi: 10.1103/PhysRevLett.33.1139.
- J. B. Taylor. Relaxation and magnetic reconnection in plasmas. *Rev. Mod. Phys.*, 58:741–763, July 1986. doi: 10.1103/RevModPhys.58.741.
- G. Valori, B. Kliem, T. Török, and V. S. Titov. Testing magnetofrictional extrapolation with the Titov-Démoulin model of solar active regions. *Astron. Astrophys.*, 519:A44, September 2010. doi: 10.1051/0004-6361/201014416.
- A. A. van Ballegoijen, E. R. Priest, and D. H. Mackay. Mean Field Model for the Formation of Filament Channels on the Sun. *Astrophys. J.*, 539: 983–994, August 2000. doi: 10.1086/309265.
- G. M. Webb, Q. Hu, B. Dasgupta, and G. P. Zank. Homotopy formulas for the magnetic vector potential and magnetic helicity: The Parker spiral interplanetary magnetic field and magnetic flux ropes. *J. Geophys. Res. (Space Phys.)*, 115:A10112, October 2010. doi: 10.1029/2010JA015513.
- L. Woltjer. A Theorem on Force-Free Magnetic Fields. *Proceedings of the National Academy of Science*, 44:489–491, June 1958. doi: 10.1073/pnas.44.6.489.
- A. R. Yeates and G. Hornig. The global distribution of magnetic helicity in the solar corona. *Astron. Astrophys.*, 594:A98, October 2016. doi: 10.1051/0004-6361/201629122.